Lab report
E217 STYX

Chenhuan Wang and Harilal Bhattarai

November 11, 2020

This is abstract.

1. Introduction

Cosmic rays physics as a frontier to discover and validate laws of physics has existed for quite some time. As early as 1912, Victor Hess already used balloon with "electrometers" to detect ionizing radiation at an altitude [1]. Nowadays, cosmic rays is a popular research area with numerous large scale experiments, such as IceCube, AMS-02, and Pierre Auger. Although cosmic rays experiments suffer from uncontrolled particles sources, its energy (up to $1 \times 10^{20}\,\mathrm{eV}$) exceed state-of-art accelerator energy (up to 13 TeV) by a large margin [2].

A large portion of cosmic rays consists of neutrinos, which have a tons of unsolved mysteries, like neutrino oscillations, origin of its mass and $\mathcal{CP}$ (even $\mathcal{CPT}$ violation [3]) violations. By studying energy spectrum of comic rays, we can look into the propagation of these particles and thus determine properties of intergalactic space [2]. Sometimes features of cosmic rays might need dark matter to make sense [4][5].

Beside all these potential intriguing problem, the setup of Styx has a rich heritage. The straw modules were formerly a part of ZEUS Straw Tube Tracker (STT) to study secondary cosmic rays [6].

This report is arranged as following. A general overview of cosmic rays is given in section 2. Electronics and schematics of the setup are shortly introduced in section 3. Before the data taking, optimal operating voltage PMT and threshold of discriminators need to be set and straws should be calibration. These are done in sections 4 and section 5. The tracking analysis is presented in section 6. Section 7 concludes this report.

2. Cosmic rays

Cosmic rays are a population of elementary particles and nuclei coming from outer space with several MeV to macroscopic energies ($\sim$ J). Energy spectra of cosmic rays follow a falling power-law (albeit with several small features) [7] [2]

$$N(E) \propto E^{-\gamma}$$

Cosmic rays of primary origin (i.e. directly from astrophysical sources without interactions) enter the earth atmosphere and they will produce the so-called secondary cosmic rays. Comparing the interaction lengths for hadronic and leptonic particles and atmosphere column density reveals that practically all cosmic rays at sea level are secondary, even tertiary [4]. All primary particles either interaction with air or decay depending on their energies. Essentially the atmosphere acts like a giant calorimeter and particle cascades are generated [4].

Most of primary cosmic rays consist of hydrogen atoms [2]. In fact, 85% are protons [4]. These protons produce mainly secondary pions and then kaons. In the end, at sea level most abundant particles with energy $> 1\,\mathrm{GeV}$ are muons (and corresponding neutrinos) [7].

There is a rather important angle dependence of muon spectra because of competition between decay and interaction. At sea level, the muon population is dominated by low energy muons (generally true for all particles). With low energy, it becomes easier for muons from inclined angle to decay and absorbed in atmosphere [4]. This can be parametrized as [4]

$$I_\mu(\theta) = I_\mu(\theta = 0)\cos^n\theta \tag{1}$$

with $n \approx 2$. Note that this formula is valid only for small zenith angle [8]. Physically, we still expect some muon flux at $\theta = \pi/2$ but equation 1 predicts zero muon flux.

Energetic particle will produce extensive shower in the atmosphere. This makes electrons and positrons quite abundant at sea level. They usually have pretty low energy, because of production mechanisms and energy losses [4].

3. Setup

3.1. Individual components

Drift chamber is a type of gaseous ionization detector. As its name suggest, it detects ionizing particles by a electric field inside. When the gas atoms get ionized, the electron will transport to the anode and generate a signal. Especially near the anode wire, the electric field is so huge that the electron becomes ionizing itself and cause further discharge. This effect is called avalanche [9]. Obviously, number of ions collected at anode depends strongly on the voltage put between anode and cathode.

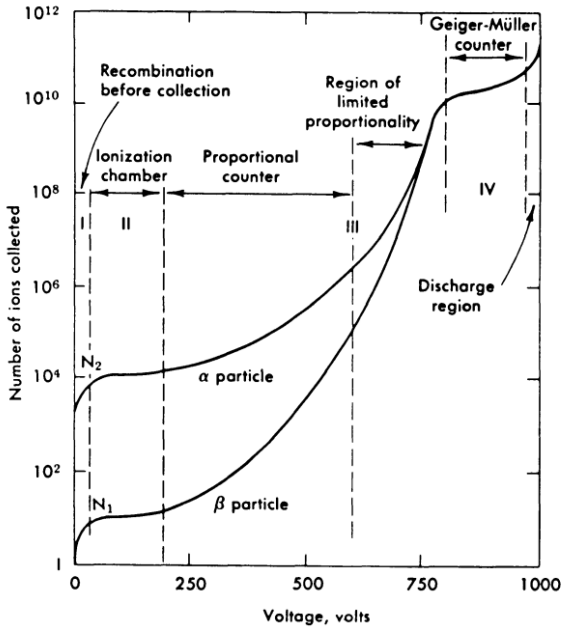

Figure 1: Example diagram of number of ions versus applied voltage in a single wire gas chamber (taken from [9]). Note that vertical axis is in logarithmic scale.

An exemplar development of number of ions with increasing voltage is shown in figure 1. In this setup, we essentially want to saturate the gas chamber (thus to region IV in figure 1) so that it can reliably count the ionizing particles regardless of their energy.

In this experiment, there are three drift chamber modules, see figure 3. In each of these, there are three layers of 88 straws [10].

Scintillator and PMT work as external trigger here. They together are able to convert ionizing particle into relatively low energy photons (scintillator), convert photon into electrons using photoelectric effect, and finally with electric field to multiply the number of electrons to generate visible signals [11]. Here two such detectors are used, one on top of the drift chamber and on below [10], see figure 3.

Shaper A shaper is a module which turns inputs pulse into logic signals of standard levels and fixed width [9].

TDC stands for Time-to-Digital Converter measures the time between two signals and gives the time difference of these two [9].

Coincidence unit determines if two or more logic signals overlap with each other within a preset time intervals and output signal if true and no signal if false. The present time is called resolving time. It can be implemented with a transmission gate or simply summing and passing through a discriminator [9].

3.2. Whole setup

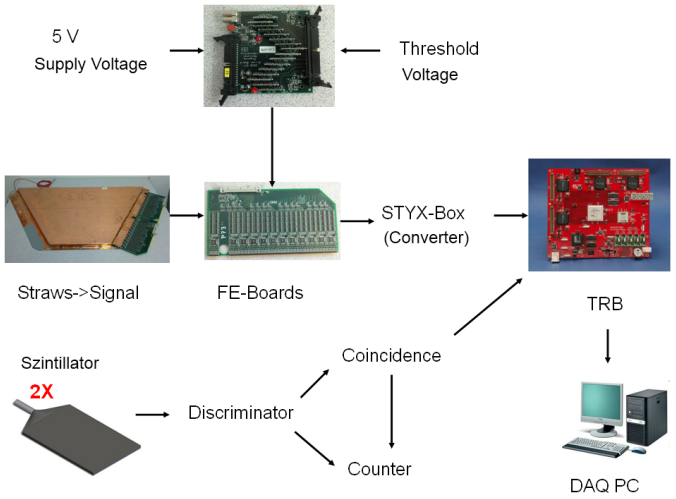

Figure 2: Schematics of the experiment setup [10].

Schematically the setup is like in figure 2. The front end boards (FE-boards) are attached to the straws. The boards contain amplifiers, shapers and discriminators, so that as long as input signal pass a set threshold, a logic signal is generated. The threshold voltage can be set on an external power supply. As for the trigger part, the signal will need to pass discriminators (to filter out noises) and goes to a coincidence unit. The coincidence unit makes sure that an event is only recorded when it flies through both scintillators. In the end, signals from straw modules and scintillator units go into TRB board and to the PC [10].

The actual setup is shown in figure 3. Straw modules with FE-boards are the copper layer between the two plastic bags, which are the triggers. Several other electronics are on the rack on the right side of figure 3.

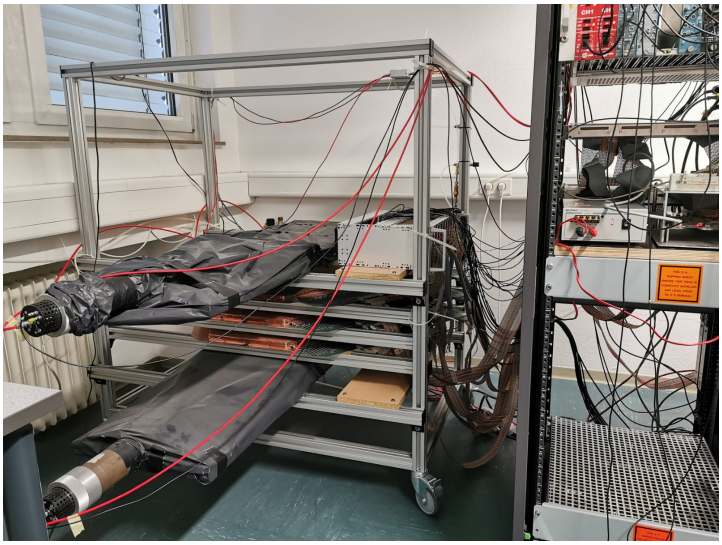

Figure 3: The actual setup

4. Voltage determination

- checked gas system is working
- PMT voltage diagram. Don't forget to compare the plot to the one in the setup.
- Include overlay and rate plots. In rate plots, it should go down. In overlay, with the right voltage, all pulses should has similar height. Just need to argue somehow why 2.0 is the right voltage.
- plots with name ok and bad are the plots in the root files. They should belong to the last bullet point. I beliebe the tutor mentioned that we don't necessarily need these plots in the report.

5. Calibration

After adjusting the PMT voltage and threshold voltage, the setup should function as expected. An overnight data taking is performed and all data has been stored. The tutor mentioned that the calibration option 1 is not working properly, so the second option is chosen.

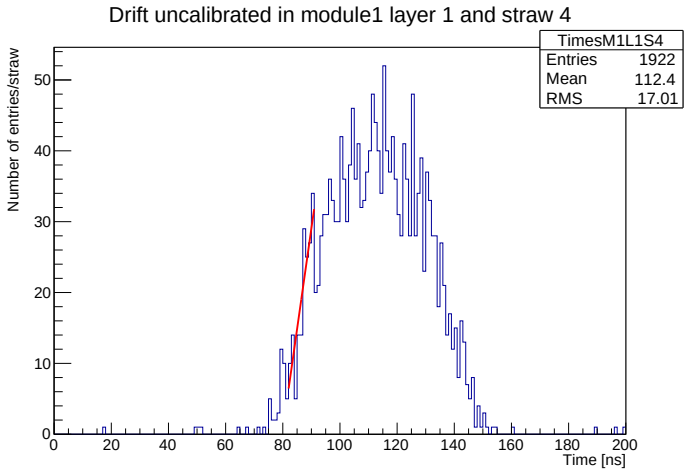

(a) Before calibration. Red line is a fit.

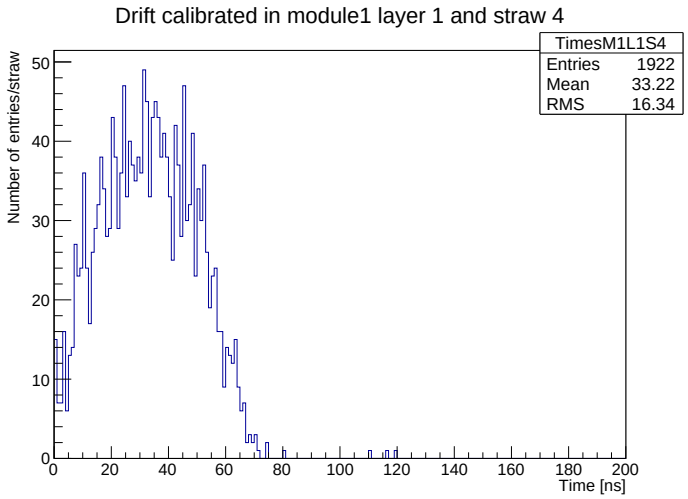

(b) After calibration

Figure 4: Drift time spectrum before and after calibration.

The calibration is done straw-by-straw using the data. One part of the data is used to map out the drift time spectrum for each straw. During the calibration, the program will try to shift the drift time, so that it starts at zero time. Exemplar spectra can be found in figure 4. During the calibration a fit is done to the ”leading” edge of the drift spectrum. The initial time t_0 is then set the intersection point of the fit line with horizontal axis.

The calibration is performed with 300 000 events using the program `StyxCalibration` (with

`--no-clean` and `--all` options). The calibration method is specified with `-A CalibStrawByStraw`. After execution of the command, corresponding `root` and `txt` file are generated.

In the generated `root` file, there are two plots of particular interest: `Uncalibrated/Layers2D` and `Calibrated/Layers2D`. These plots show the drift spectra for each straw in one particular module and layer before and after calibration. Some examples are figure 5, 6, and 7.

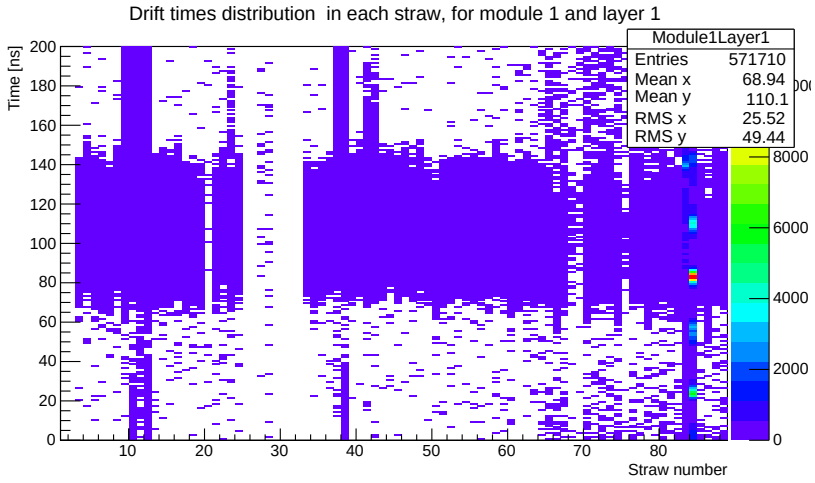

(a) Before calibration.

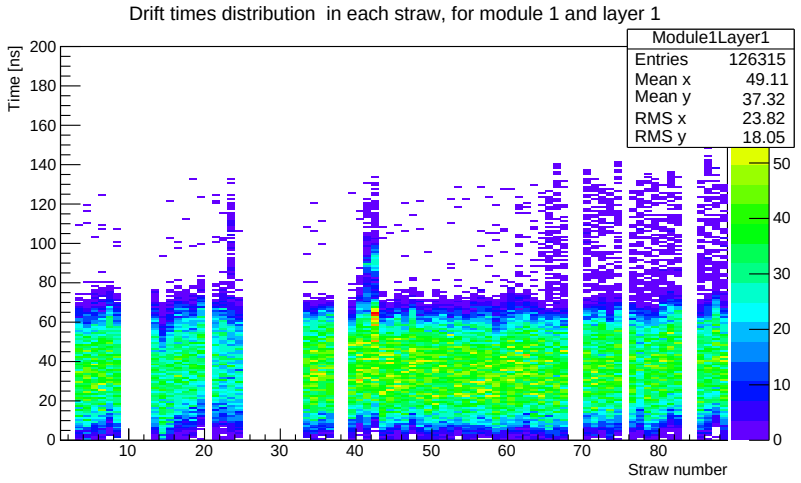

(b) After calibration

Figure 5: Drift time spectra for all straws in module 1 and layer 1 before and after calibration.

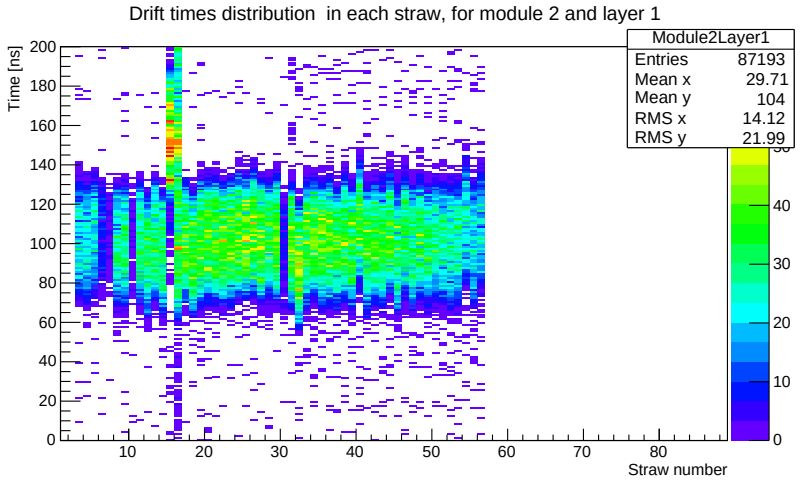

(a) Before calibration.

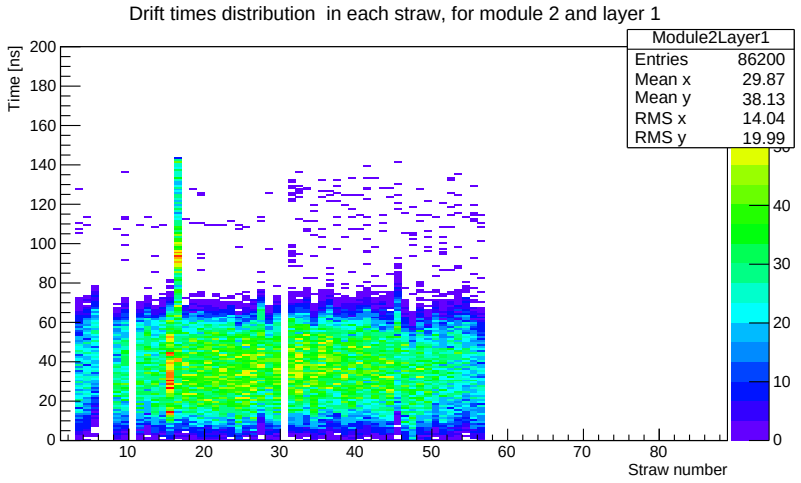

(b) After calibration

Figure 6: Drift time spectra for all straws in module 2 and layer 1 before and after calibration.

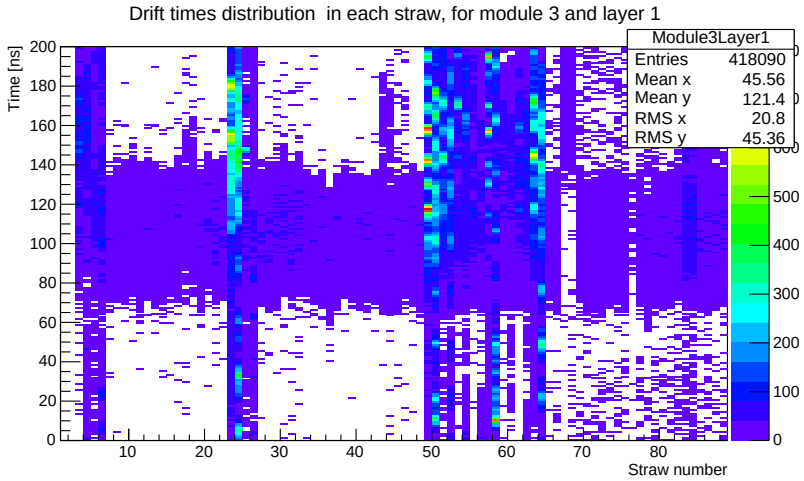

(a) Before calibration.

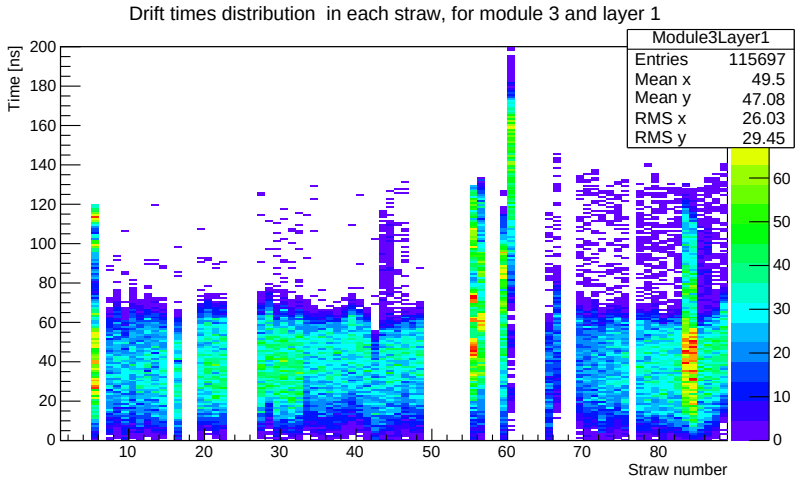

(b) After calibration

Figure 7: Drift time spectra for all straws in module 3 and layer 1 before and after calibration.

By comparison of these plots, we see that the calibration works normally for most straws. Before the calibration, there are no particular "hot" time (interval of time with clear peak in event counts) and events are rather scattered in time. But after, events are properly aligned with each other and there is a clear peak at $t \approx 40\,\text{ns}$. One can also notice that some straws don't have a lot of outputs or even no output at all. These straws should be marked as "dead". Sometimes, even after calibration, the drift spectra cannot get into the shape we expect, such as straw 15 16 in figure 6. This can be understood as the calibration doesn't behave well. The exact reason of failing calibration is still yet unknown. These certainly should not be used for the track analysis and these straws are marked as "hot" or "continuous".

The aforementioned labels to each straws can be mapped onto the cross section of the detectors, see figure 8.

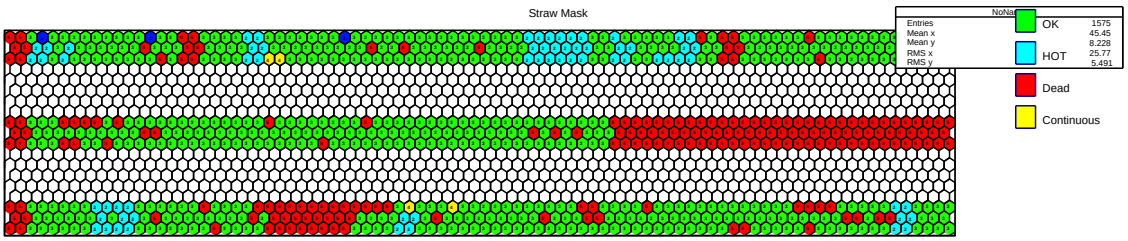

Figure 8: Straw masks. Note that the numbering should start from bottom. It means that the bottom module is module 1, the same for layer numbering. Dead straws are in orange.

With the masks, one can even simulate the events. By looking at it, we are able to gain further insight to the reconstruction process (algorithms). For example, with number of events at 20 and number of tracks at 3, one has figure 9. In the figure, red circles should be the expected position of the track only using one straw on one layer. When signals get correlated in the same module, possible tracks (green line) can be drawn. Then the signals from all three modules get combined together and a clear track (blue dotted lines) can be reconstructed.

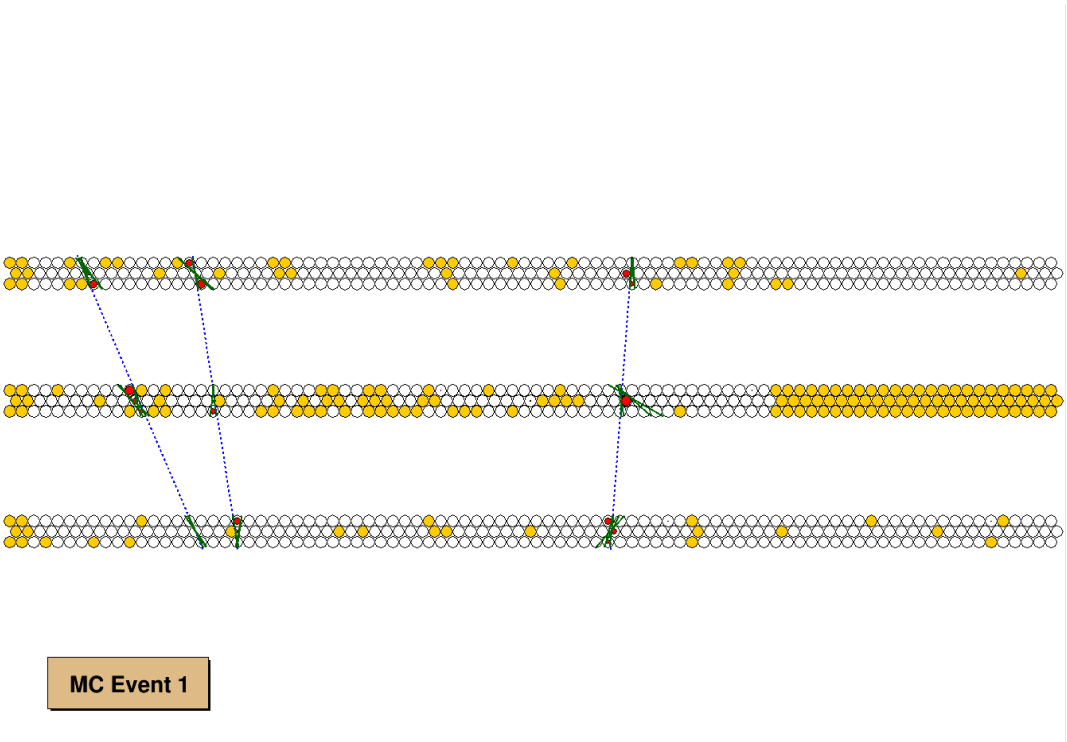

Figure 9: Simulation of events with `Nevents=20` and `Ntracks=3`. Orange straws are the straws marked as "dead".

6. Tracking analysis

Now we have the straws are calibrated with the 300 000 events, we want to reconstruct other 200 000 events with `StyxM2C2` (of course with calibration applied). The program `StyxLabCourse` is used for the analysis. It contains a class `StudentAnalysis`, where extra code can be inserted to analyze the data. Since the its methods are called for every event, it becomes easier to store some rudimentary histograms to `root` files first and use macro to draw rather complicated histograms.

One can inspect the number of hits for each layer in one module. For example, the plot of bottom module is figure 10. It is expected that the three histograms have similar shapes, considering there physical vicinity. The shapes originate from the geometry of the detectors: some straws are just longer than others, resulting more hits.

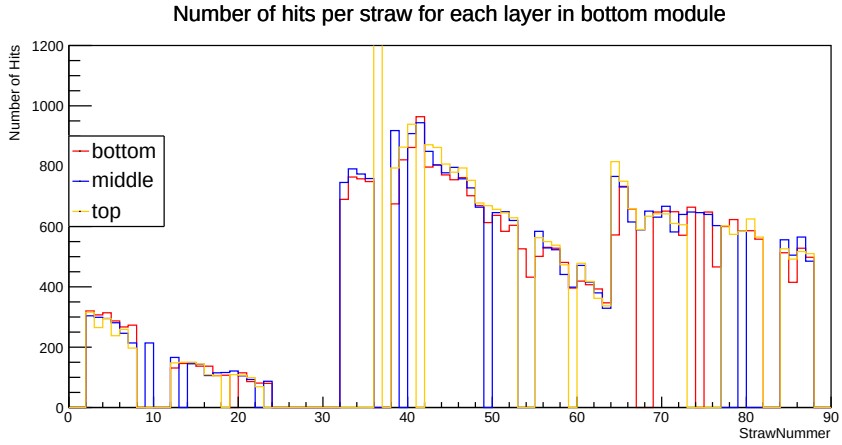

Figure 10: Number of hits per straws for each layer in bottom module

Comparison of total numbers of hits in modules is potentially interesting as well. Figure 11 shows the total number of hits in bottom and top modules. They have similar shapes in some regions, but quite different in some other regions. This can be caused by the "qualities" of straws, i.e. positions of dead and hot straws on the modules don't match each other.

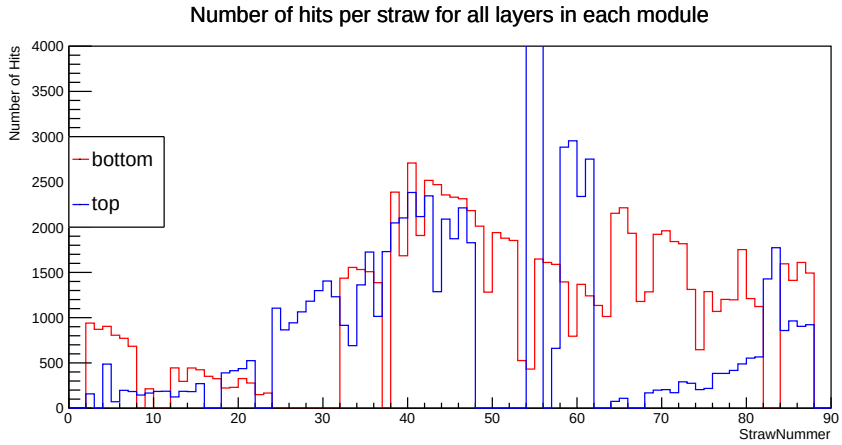

Figure 11: Number of hits per straws for all layers in bottom and top module

Figure 12 shows the correlation between number of tracks and number of hits of an event. According to [12], lower limit of a bin is included and upper limit is excluded (it becomes lower limit for the next bin).

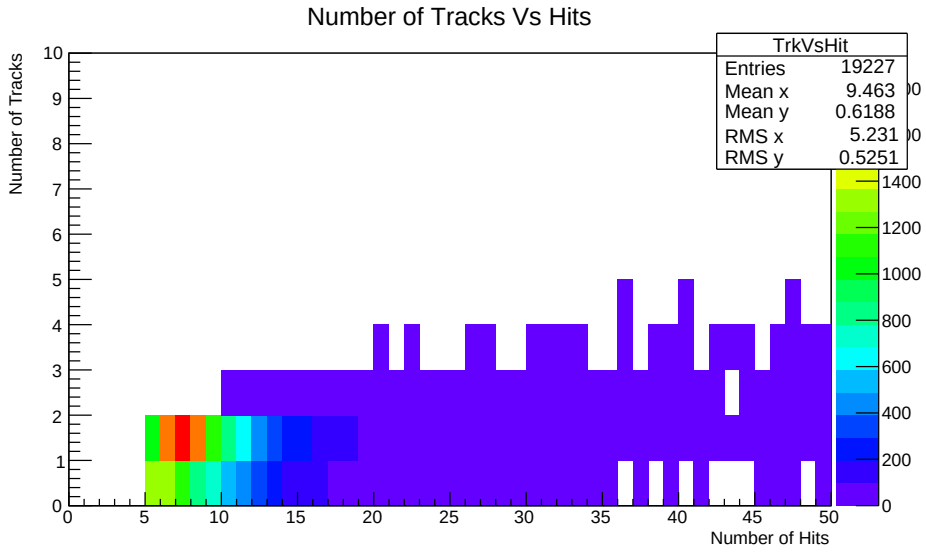

Figure 12: Number of tracks against number of hits

There are two clear sharp edges with number of hits at 5 and 10 and a couple of more subtle ones with number of hits at 20 and $\sim$ 35. Thus the interpretation of the plot in figure 12 is that the reconstruction algorithm probably demand minimal 5 hits for every track. This "rule" breaks down at high number of hits, probably because that an event with high number of tracks is not very likely.

A obvious "hot" region in figure 12 has number of tracks at 1 and number of hits ~ 7. Thus most events have only 1 track and ~ 7 hits registered. One can try to imagine the distribution projected to horizontal axis, i.e. an one-dimensional histogram of number of hits. It resembles a shape of Poisson distribution (with a lower cutoff of course), which is characteristic for a counting experiment.

Angular (zenith angle) distribution of events with one track is shown in figure 13. It (presumably) is because of limitation of the reconstruction program that only one zenith angle can be stored for one event. This cut will not in theory create a bias in the angular distribution, since there is no reason to believe that multiple tracks in one events are correlated in any way. There is an ambiguity in the data, namely the definition of `track slope` used in the program. We interpreted it as the plain slope instead of the angle, so that the zenith angle is calculated with arctan function. Either way, the "choice" of the definition has virtually no impact on the angular distribution and following fit.

Basic features of figure 13 are sort of expected. It peaks at zero zenith angle, since decay probability starts to increase with the angle, see equation 1. A closer look reveals that the histogram is as we expect. A fit is done

$$f(x) = A\cos^n x$$

between $\theta = -0.5$ and $\theta = 0.5$, since at large angle the $\cos^2$ doesn't apply anymore. A and n

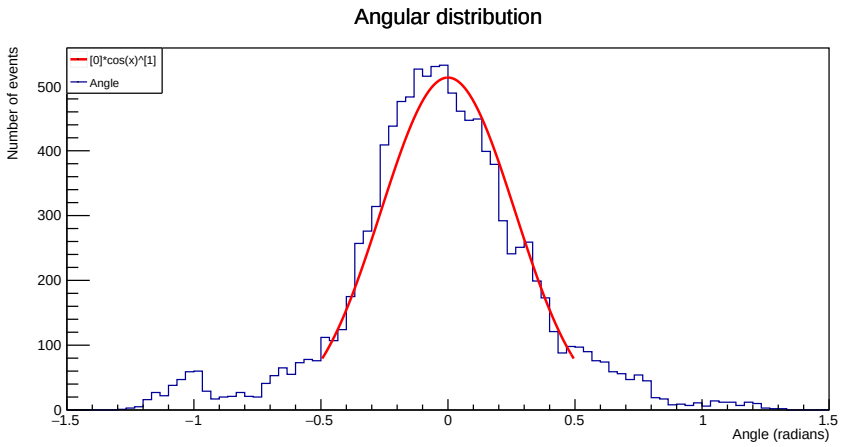

Figure 13: Angular distribution of events with a single track

are the fit parameters, which are determined as

$$A = 513.00 \pm 6.95$$
$$n = 14.59 \pm 0.35$$

The interval of zenith angle can certainly be adjusted to influence the quality of the fit. But we reckon that our choice should cover the region that distribution is supposed to follow equation 1 and some changes don't really affect results too much anyway.

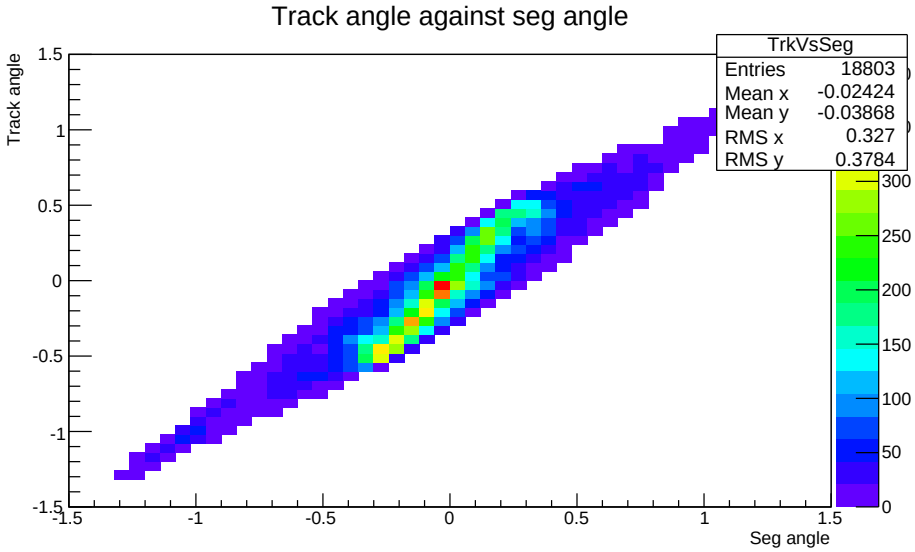

Figure 14: Zenith (track) angle against segment angle.

Another plot worth investigating is zenith angle (track angle) against segment angle for events with one track, see figure 14. Segment angle, we suppose, denotes the angle of the "track" in only one module. In theory they should match perfectly. But we need to consider detector space/angle resolution, so that the distribution is smeared. Figure 14 is almost what

we want to see, except the central "hot" regions is inclined a bit and thus the plot is not symmetric along 45° line.

7. Conclusion

After two days' effort, StyX is properly setup. Calibration masks match with number of hits per straw quite well. In other word, calibration works. But in the end, the overall result is borderline satisfactory.

Distribution of events on two-dimensional plane of segment angle and track angle is a bit odd. Ideally, we have symmetric distribution even considering resolution. This likely have something to do with the reconstruction algorithm or even the geometry of the setup. Since both subjects are not main focus of this report, we will not go deep and try to speculate the exact problem(s).

The goal of the experiment is to obtain the angular distribution of atmospheric muons. The distribution doesn't agree with theory. The value of n deviate from the theory quite a lot ($\sim 35\sigma$ away). Statistical error can certainly be excluded. It is highly unlikely that the theory is faulty here, since some other more sophisticated and advanced experiments have $n \approx 2$ [13][8]. Then we only have setup or reconstruction method to blame. Again we are not familiar with the reconstruction so no further speculations.

The geometry of the detectors are certainly a factor here. Figure 3 shows that the trigger systems are stacked directly over and under the straw modules. One problem is that in the electronics we demand both PMT must have signals in order to record the events (coincidence). This produces a bias in the data, in the sense that once the incident angle is relatively large, the events might not get recorded. At large incidence angle, the particles could very like only fly through one PMT or even none of both PMTs (though in this case the angle must be quite large so that $\cos^2$ law is broken anyway). But particles directly from vertical direction are detected as expected. Eventually this distorts the distribution in a way that fluxes around $\theta = 0°$ is untouched but the fluxes at larger angles get suppressed.

A possible future improvement could be just use one PMT as a trigger or these two PMT on one side of straw modules. It will increase noise level but it can presumably improve the distorted angular distribution.

A. Appendix

References

[1] Prof. H. Pleijel. *Award ceremony speech*. URL: https://www.nobelprize.org/prizes/physics/1936/ceremony-speech/.

[2] Thomas K. Gaiser, Ralph Engel, and Elisa Resconi. *Cosmic rays and particle physics*. Cambridge university press, 2016.

[3] Gabriela Barenboim and Jordi Salvado. "Cosmology and CPT violating neutrinos". In: *The European Physical Journal C* 77.11 (Nov. 2017). ISSN: 1434-6052. DOI: 10.1140/epjc/s10052-017-5347-y. URL: http://dx.doi.org/10.1140/epjc/s10052-017-5347-y.

[4] Claus Grupen et al. *Astroparticle physics*. Springer, 2005.

[5] D.M. Gomez Coral and Arturo Menchaca-Rocha. "SM antideuteron background to indirect dark matter signals in galactic cosmic rays". In: *Journal of Physics: Conference Series* 1602 (July 2020), p. 012005. ISSN: 1742-6596. DOI: 10.1088/1742-6596/1602/1/012005. URL: http://dx.doi.org/10.1088/1742-6596/1602/1/012005.

[6] *Straw Tube Young Student eXperiment - STYX*. URL: https://www.brock.physik.uni-bonn.de/research/styx-experiment.

[7] P.A. Zyla et al. "Review of Particle Physics". In: *PTEP* 2020.8 (2020), p. 083C01. DOI: 10.1093/ptep/ptaa104.

[8] Prashant Shukla and Sundaresh Sankrith. "Energy and angular distributions of atmospheric muons at the Earth". In: *Int. J. Mod. Phys. A* 33.30 (2018), p. 1850175. DOI: 10.1142/S0217751X18501750. arXiv: 1606.06907 [hep-ph].

[9] William R. Leo. *Techniques for nuclear and particle physics experiments*. 2nd. Springer-Verlag Berlin Heidelberg GmbH, 1994.

[10] Unknown. "Lab manual. E217 STYX". In: (2020).

[11] Hermann Kolanoski and Nobert Wermes. *Teilchendetektoren: Grundlagen und Anwendungen*. Springer. ISBN: 978-3-662-45350-6.

[12] CERN. *User Guide: Histograms*. URL: https://root.cern.ch/root/htmldoc/guides/users-guide/Histograms.html.

[13] M. Bahmanabadi. "A method for determining the angular distribution of atmospheric muons using a cosmic ray telescope". In: *Nuclear Instruments and Methods in Physics Research Section A: Accelerators, Spectrometers, Detectors and Associated Equipment* 916 (2019), pp. 1–7. ISSN: 0168-9002. DOI: https://doi.org/10.1016/j.nima.2018.11.010. URL: http://www.sciencedirect.com/science/article/pii/S0168900218315560.